Available online at http://scik.org
Commun. Math. Biol. Neurosci. 2024, 2024:51
https://doi.org/10.28919/cmbn/8518
ISSN: 2052-2541

COMPARATIVE ANALYSIS OF CONTROL INTERVENTIONS: SURVIVAL ANALYSIS AND INDIVIDUAL-LEVEL SIR MODEL APPROACH

BIDAH SARA[1,2], CHAYOUKH OUSSAMA[1], KADI MAROUANE[1], BOUTAYEB HAMZA[1], ZAKARY OMAR[1,*]

[1]Laboratory of Analysis, Modeling and Simulation, Faculty of Sciences Ben M'Sik, University Hassan II of Casablanca, Morocco

[2]Biology and Health Laboratory, Faculty of Sciences Ben M'SIK, Hassan II University of Casablanca, Morocco

Abstract. This study introduces a novel approach to assess the effectiveness of two distinct control strategies, utilizing non-pharmaceutical interventions and treatment measures as exemplars. Focused on understanding infectious disease dynamics within closely-interacting communities such as the Hajj pilgrimage or summer camps, meticulous surveillance is employed to monitor infection, recovery, and vulnerability rates. Leveraging this data, a mathematical model is calibrated to precisely estimate parameters. Through numerical simulations, the impact of the two control strategies is evaluated. Results demonstrate significant reductions in infection rates with both approaches, with treatment measures exhibiting a more pronounced effect. Survival analysis underscores expedited recovery times associated with treatment, indicating its superior efficacy in containing infection spread. Statistical comparisons substantiate the practical significance of treatment interventions in enhancing survival outcomes within the studied groups. Despite inherent assumptions, this study provides valuable insights into the comparative effectiveness of diverse control measures in managing infectious diseases within communal living environments. The proposed approach offers a framework for systematic evaluation and comparison of control strategies, contributing to the development of more effective disease management protocols.

*Corresponding author
E-mail address: zakaryma@gmail.com
Received March 03, 2024

Keywords: medical treatment; non-pharmaceutical; control strategies; individual-level SIR model; survival analysis; Kaplan-Meier curves; Log-rank test; cohort study.

2020 AMS Subject Classification: 92B05, 92D30, 65C60, 92D25.

1. INTRODUCTION

In the realm of global public health, combatting infectious diseases presents a formidable challenge, necessitating the creation and refinement of effective intervention techniques [1, 2]. Understanding the intricate dynamics of susceptible, infected, and recovered individuals in a population is crucial in grappling with this challenge, and the use of dynamic epidemiological models plays a crucial role in this endeavor. Recent progress in mathematical modeling has facilitated the exploration of various control measures aimed at curtailing the dissemination of infectious agents [3, 2].

The development of new mathematical models is pivotal in enhancing our comprehension of infectious diseases, particularly in the context of pandemics [4, 2, 5, 3]. These models enable researchers to simulate and scrutinize complex interactions between individuals within a population, shedding light on disease transmission dynamics. The ongoing refinement of these models significantly contributes to the identification and assessment of innovative disease control strategies [6]. By incorporating real-world data and adapting to evolving scenarios, these models aid policymakers and public health officials in devising effective interventions, optimizing resource allocation, and ultimately lessening the impact of infectious diseases like COVID-19 on a global scale [7, 5].

In a particular study [8], the authors delve into the factors influencing the risk of infection among individuals exposed to a tuberculosis case. Key determinants include the infectivity of the source case, the level of exposure experienced by susceptible individuals, and the susceptibility of the person to infection. The infectivity of the source case is influenced by factors such as cough frequency, sputum bacilli density, and microbial virulence. Previous research suggests that sputum-smear-positive pulmonary tuberculosis cases are more likely to infect their contacts compared to sputum-smear-negative cases. The degree of exposure hinges on the proximity of contact between a susceptible individual and the infectious tuberculosis case.

In another study [9], the authors explore the dynamics of infectious disease spread within person-to-person contact networks, focusing on factors beyond the number of contacts an individual has. They analyze clustering, variations in infectiousness or susceptibility, and closeness of contacts. Utilizing analytical techniques and validation with a realistic social network, the research finds that clustering primarily influences the growth rate, infectiousness heterogeneity affects the probability of an epidemic, and susceptibility heterogeneity controls the epidemic size.

This study builds upon the foundational framework of the Susceptible-Infectious-Recovered (SIR) model, widely used in epidemiology [7, 4, 1, 6, 10, 11]. By integrating individual-level dynamics and control interventions, the aim is to illuminate the impact of targeted medical treatments and non-pharmaceutical interventions on the progression and containment of infectious diseases. The investigation delves into the nuanced effectiveness of two distinct control strategies representing medical treatments and measures focused on reducing interpersonal contact [5, 12, 13].

Incorporating real-life situations such as the Hajj period, training camps, and summer camps, where living in close quarters can heighten the risk of disease transmission, we replicate the dynamics of infectious diseases within communities. By continuously monitoring and gathering data, our objective is to estimate critical parameters like vulnerability rates, infection rates, and recovery rates, offering insights that can guide evidence-based public health interventions.

The Kaplan-Meier survival curve is a visual tool commonly utilized in survival analysis to predict the likelihood of an event, such as recovery or survival, over time [14, 15, 16]. It is especially beneficial when examining time-to-event data, where the timing of an event is of interest [14]. This curve is formulated by computing the survival probability at each observed event time point. It takes the form of a step function that diminishes at each event time, signifying the occurrence of the event. The event under consideration may vary depending on the study. In infectious disease modeling, it may signify recovery, while in other contexts, it could denote death, relapse, or any other pertinent event [17].

In survival analysis, some individuals may not undergo the event during the study period. In such instances, their data is considered censored. The Kaplan-Meier estimator incorporates censored data, adjusting the survival probabilities accordingly [17].

The log-rank test yields valuable insights into the efficacy of different control strategies in influencing the survival outcomes of individuals [18]. The interpretation of the results will steer our comprehension of which control measures demonstrate a substantial impact on reducing the duration of infectiousness. Furthermore, these findings contribute to the identification of optimal strategies for mitigating the spread of infectious diseases within specific populations [19].

2. Materials and Methods

We undertake a thorough investigation involving a cohort of n individuals living together over the course of the study. This group, reminiscent of various real-life scenarios such as the Hajj pilgrimage, training camps, or summer camps, serves as an example of a communal living environment conducive to the continuous and uninterrupted monitoring of infectious disease dynamics. Situations like the Hajj period, characterized by large gatherings, and training and summer camps with communal living arrangements, elevate the potential for disease transmission.

In our research, we employ a rigorous and persistent surveillance approach. This ongoing monitoring involves carefully tracking each individual's infection rate, recovery rate, and vulnerability rate over time. Through this method, our goal is to capture the intricate dynamics of disease spread within this closely-knit community. The duration of the study allows for the comprehensive collection of detailed data for each person, providing a thorough depiction of their susceptibility to infection, disease progression, and eventual recovery.

The data gathered during this monitoring period forms the foundation for parameter estimation in our mathematical model. By utilizing the observed infection, recovery, and vulnerability rates for each individual, we utilize statistical techniques to adjust the model parameters. This calibration process entails refining the model to align with real-world data, enabling us to derive precise and context-specific estimates for parameters such as transmission rates and recovery

rates. Essentially, this iterative approach integrates empirical observations with mathematical modeling, resulting in a robust framework that mirrors the dynamics of infectious diseases within a closely-interacting community.

3. Model Description

In our mathematical framework, the susceptibility rate $(S_{j,i})$ emerges as a crucial parameter delineating an individual's vulnerability to infection at a specific temporal point i. This measure is intricately influenced by various factors including immunological profile, genetic disposition, and past exposure history [8]. A heightened susceptibility rate signifies an increased predisposition to infection, underscoring the potential for rapid disease dissemination within the populace. Monitoring individual susceptibility rates is imperative for infectious disease studies, public health strategizing, and the formulation of efficacious intervention tactics. Quantifying susceptibility rates offers valuable insights into disease transmission dynamics and the efficacy of preventive measures such as vaccination campaigns or awareness drives [20].

Simultaneously, the infection rate $(I_{j,i})$ serves as a pivotal gauge, capturing the degree of infection in an individual j at a given moment i. This parameter encapsulates the dynamic interplay between the individual's immune response and the pathogen. A higher infection rate signals a more pronounced presence of the infectious agent within the individual, indicating an escalated risk of disease progression and potential transmission to others. Monitoring individual infection rates enables healthcare practitioners to evaluate disease severity, tailor suitable treatment approaches, and implement targeted public health interventions to mitigate further transmission [21, 8]. Integration of individual infection rates into our model furnishes a nuanced understanding of disease progression for specific individuals, contributing to a comprehensive comprehension of the overall epidemiological panorama.

Complementary to these facets, the recovery rate $(R_{j,i})$ stands as a pivotal measure denoting the fraction of individuals j recuperating from infection at a specific time i. This metric is assessed not only through the resolution of clinical manifestations but also by monitoring immunological indicators such as the presence of specific antibodies. Symptom resolution indicates functional recuperation, while the detection of specific antibodies confirms a successful adaptive immune response [22]. The decline in infection rate, coupled with heightened antibody

levels, serves as indicators of progression towards recovery. These combined markers furnish a holistic perspective on individuals' recovery trajectories, aiding healthcare professionals in gauging treatment efficacy and tracking immune response dynamics. Understanding recovery rates at the individual level contributes to refining clinical interventions and devising targeted public health strategies to facilitate optimal recovery [23].

Individuals commence in a susceptible state, signifying their vulnerability to the infectious agent due to factors such as lack of immunity, genetic predisposition, or exposure history.

When an individual j encounters an infectious individual k, the likelihood of transmitting the infection from k to j is characterized by a transmission rate denoted as β_j. This rate hinges on the interplay between the susceptibility of individual j and the infectiousness of person k. Individual susceptibility reflects their vulnerability to the infectious agent, while the infectiousness of the source individual influences the potential for transmission. This interaction is mathematically modeled using the standard contact term in the SIR model, wherein $\frac{\beta_j S_{j,i} I_{j,i}}{N_{j,i}}$ signifies the probability of transmission during their interaction. This results in the additional production of pathogens, contributing to an elevation in viral load within individual j and further influencing infection progression.

As the infection progresses, the individual's immune system dynamically responds to combat the pathogen. The recovery process $(R_{j,i})$ unfolds as the immune response effectively controls and eradicates the infectious agent, with this natural control governed by a recovery rate denoted as γ_j. This phase is marked by the alleviation and resolution of symptoms, indicative of the immune system's triumph over the infection. Moreover, recovery is accompanied by immunity development facilitated by the generation of specific antibodies tailored to combat the encountered pathogen. These antibodies play a pivotal role in providing heightened defense against potential reinfection.

We also consider two control strategies: the first, u_1, entails treatment control involving the administration of medical interventions such as antiviral drugs or antibiotics. This control aims to either directly target the infectious agent or bolster the host's immune response. Antivirals may inhibit viral replication, while antibiotics can target bacterial infections. Timely administration of these treatments can reduce the viral or bacterial load in individual j at a rate $u_{1,j,i} I_{j,i}$,

thereby expediting recovery. The second control strategy, u_2, involves non-pharmaceutical interventions or behavioral measures aimed at curtailing disease spread without relying on medical treatments. These controls are often implemented to minimize person-to-person transmission, limit exposure to the infectious agent, and promote adherence to preventive measures such as social distancing, hygiene practices, and public awareness campaigns, etc.

Considering all these factors, we outline our mathematical model in the following manner:

$$\begin{cases} S_{j,i+1} = S_{j,i} - \left(1 - u_{2,j,i}\right) \dfrac{\beta_j S_{j,i} \sum_{k=1;k\neq j}^{n} I_{k,i}}{N_{j,i}} \\ I_{j,i+1} = I_{j,i} + \left(1 - u_{2,j,i}\right) \dfrac{\beta_j S_{j,i} \sum_{k=1;k\neq j}^{n} I_{k,i}}{N_{j,i}} - \gamma_j I_{j,i} - u_{1,j,i} I_{j,i} \\ R_{j,i+1} = R_{j,i} + \gamma_j I_{j,i} + u_{1,j,i} I_{j,i} \end{cases}$$

Where $N_{j,i} = S_{j,i} + I_{j,i} + R_{j,i}$ and $S_{j,0}, I_{j,0}$ and $R_{j,0}$ are given for $j = 1, \ldots, n$, and n is the number of individuals under study. $u_{1,j,i}$ represents the effect of the first control strategy on the individual j at instant i, and $u_{2,j,i}$ represents the effect of the second control strategy on the individual j at time i.

4. Data Generation and Preparation

In this phase of our study, we outline the essential procedures for gathering and organizing the data.

4.1. Data Collection. The first step involves the identification and characterization of the pathogen by medical experts. Following this, the vulnerability, infection, and recovery rates are defined. The vulnerability rate takes into account individual-specific factors such as immunological status, genetic predisposition, and exposure history that determine an individual's susceptibility to the infectious agent at any given time. Detailed data on each individual's infection progression and recovery journey is initiated by monitoring the resolution of symptoms and the development of specific antibodies, allowing for the quantification of the infection and recovery rates.

Subsequently, the study period is carefully determined to ensure a comprehensive observation of disease dynamics over time. Factors such as the pathogen's incubation period and the

anticipated duration of individual infectiousness contribute to establishing an optimal study time-frame.

Lastly, by establishing $I_{\min}$ as the point where symptoms begin to manifest in individuals, we can determine when someone becomes infectious. This threshold helps us classify individuals as potentially contagious, enabling us to understand the average infection rate at which an infected person starts spreading the disease.

4.2. Data Preparation. In this stage, sophisticated methodologies such as non-linear regression and non-linear least squares techniques are employed, augmented by the Levenberg-Marquardt algorithm. Non-linear regression serves a crucial role in fitting the intricate dynamics of susceptibility $(S_{j,i})$, infection $(I_{j,i})$, and recovery $(R_{j,i})$ rates to observed data. This approach allows for modeling complex relationships and capturing the inherent non-linear dependencies present in infectious disease dynamics. Furthermore, the non-linear least squares method aims to minimize the sum of squared differences between observed and model-predicted values, thereby improving the accuracy of parameter estimates. The Levenberg-Marquardt algorithm refines this estimation process by balancing between gradient descent and Gauss-Newton methods. Collectively, these methodologies empower the model to effectively navigate the complexities of infectious disease dynamics, resulting in precise parameter estimates that closely align with real-world observations.

To generate data for survival analysis from the calibrated model, the infection rate parameter $(I_{j,i})$ serves as a critical determinant. The objective is to identify time points when individual infection rates drop below the predefined infection rate threshold $I_{\min}$, indicating the transition to a non-infectious state. The survival time for each individual is then computed as the duration from when they surpass $I_{\min}$ until they achieve recovery.

Finally, a dataset is compiled for survival analysis, encompassing individual-specific survival times, indicators of recovery status (event occurrence), and pertinent covariates.

5. Numerical Simulations and Discussion

5.1. Numerical simulation.

FIGURE 2. Simulation of the model for the group 2 without controls

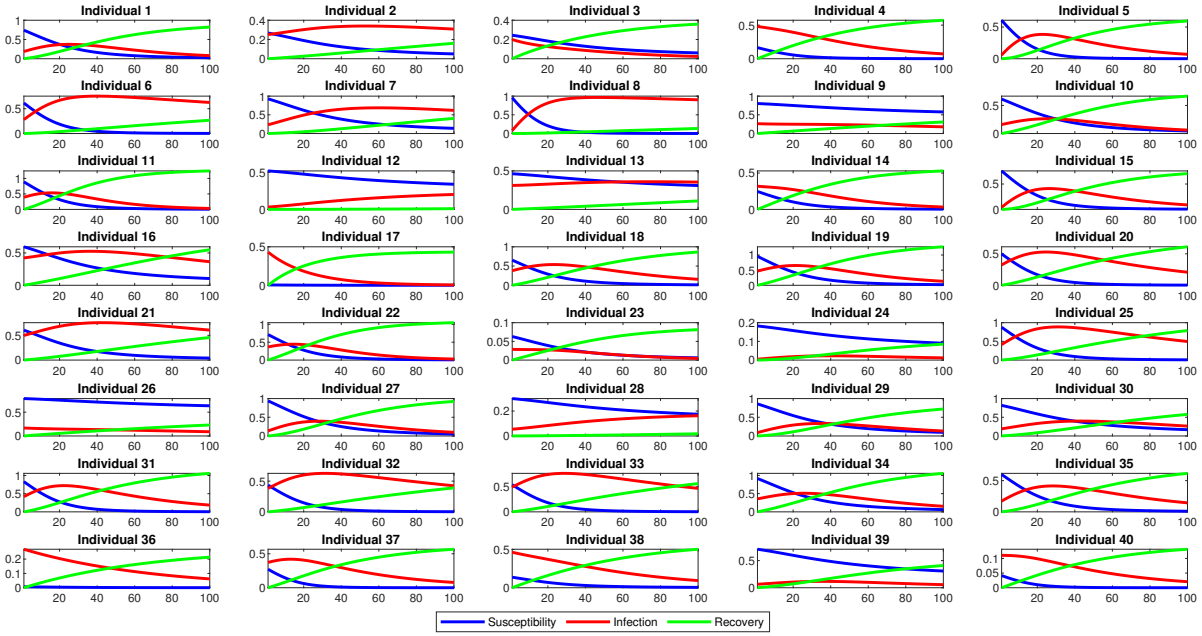

FIGURE 1. Simulation of the model for the group 1 without controls

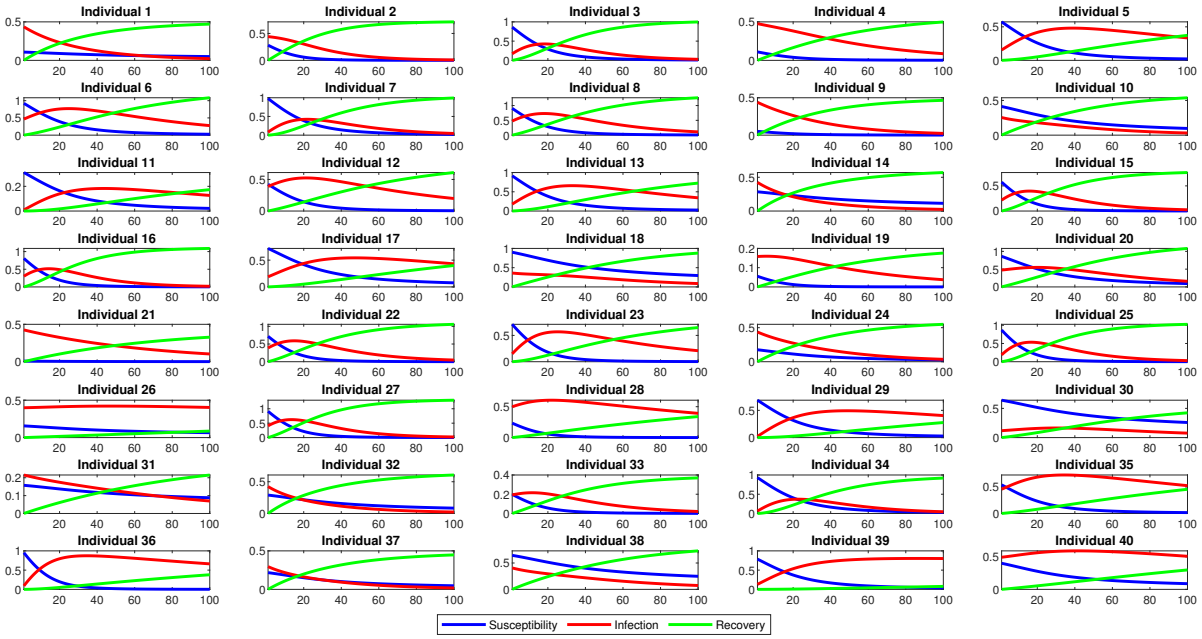

TABLE 1. Generated survival analysis data without controls for the group 1 and 2

Individual IDs	Group 1		Group 2	
	Time To Recovery	Recovery Status	Time To Recovery	Recovery Status
1	48	1	92	1
2	48	1	100	0
3	68	1	33	1
4	93	1	86	1
5	100	0	1	1
6	100	0	100	0
7	1	1	100	0
8	100	0	1	1
9	53	1	100	0
10	50	1	81	1
11	1	1	73	1
12	100	0	1	1
13	100	0	100	0
14	45	1	63	1
15	65	1	1	1
16	63	1	100	0
17	100	0	34	1
18	93	1	100	0
19	46	1	100	0
20	100	0	100	0
21	100	0	100	0
22	79	1	70	1
23	100	0	1	1
24	61	1	1	1
25	71	1	100	0
26	100	0	86	1
27	67	1	100	1
28	100	0	1	1
29	1	1	1	1
30	82	1	100	0
31	71	1	100	0
32	45	1	100	0
33	50	1	100	0
34	1	1	100	0
35	100	0	100	0
36	1	1	68	1
37	38	1	90	1
38	84	1	97	1
39	100	0	1	1
40	100	0	20	1

FIGURE 3. Survival curves without controls (a) group 1 (b) group 2

(a)

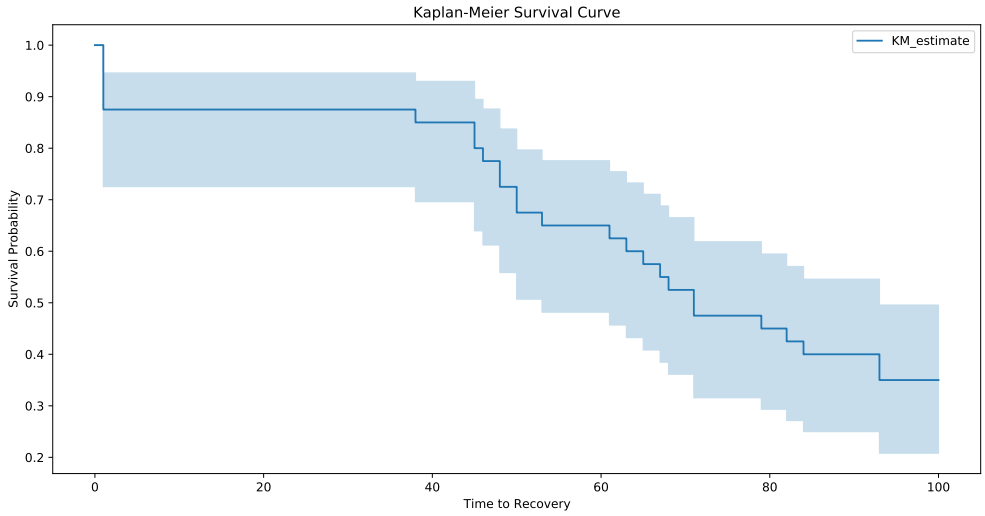

(b)

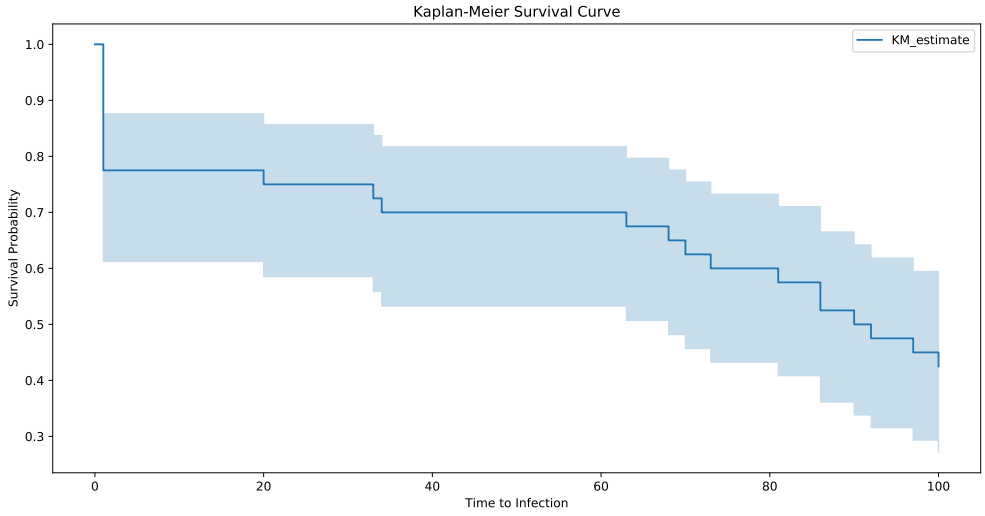

In this simulation study, we examine a population of 240 individuals divided into two groups, Group 1 and Group 2, each consisting of 120 individuals. Within each group, individuals are further divided into three subgroups, each comprising 40 people. The simulation investigates how various control strategies affect infection spread within each subgroup. For consistency, we set $I_{\min}$ to 10%

The initial 40 individuals in each group undergo the simulation without any specific control measures (referred to as $\mathbf{G}_1$ without and $\mathbf{G}_2$ without).

The next set of 40 individuals in each group undergo a control labeled u_1, representing an intervention like medical treatment or therapeutic measures aimed at reducing infection severity and duration (referred to as $\mathbf{G}_1$ with u_1 and $\mathbf{G}_2$ with u_1).

The final 40 individuals in each group are subject to a separation and awareness control, denoted as u_2, focused on reducing interpersonal contacts and increasing awareness about precautions to limit infection spread by minimizing interactions (referred to as $\mathbf{G}_1$ with u_2 and $\mathbf{G}_2$ with u_2).

For each simulation scenario (no controls, with u_1, with u_2), data is generated to record infection, recovery, and vulnerability rates for each individual, forming the basis for survival analysis.

Kaplan-Meier survival curves are constructed to visually depict the time until recovery occurs (event) in each subgroup under different control strategies. These curves visually represent the proportion of individuals who have not experienced the event up to each time point, with a steeper decline indicating a higher event rate.

Survival curves are commonly used to compare survival experiences between different groups, such as those with or without a specific treatment or control, providing insights into the effectiveness of each control measure in preventing or delaying infection. The estimated median survival time, indicated by the point where the Kaplan-Meier curve crosses the 0.5 probability mark, represents the time by which half of the individuals have experienced the event.

The main aim of this study is to compare and assess the effectiveness of three scenarios in controlling the spread of infection within the population. By analyzing the survival curves, we seek to determine which control strategy has the most significant impact on managing the infection.

Figures 1, 2, 4, 5, 7, and 8 provide an in-depth analysis of the dynamics of susceptibility, infection, and recovery rates for subgroups of 40 individuals in Group 1 and Group 2. The X-axis represents the time steps, while the Y-axis shows the rates as percentages. The Blue Line denotes the Susceptibility rate over time, the Red Line represents the Infection rate over time, and the Green Line illustrates the Recovery rate over time.

FIGURE 4. Simulation of the model for the group 1 with the control 1

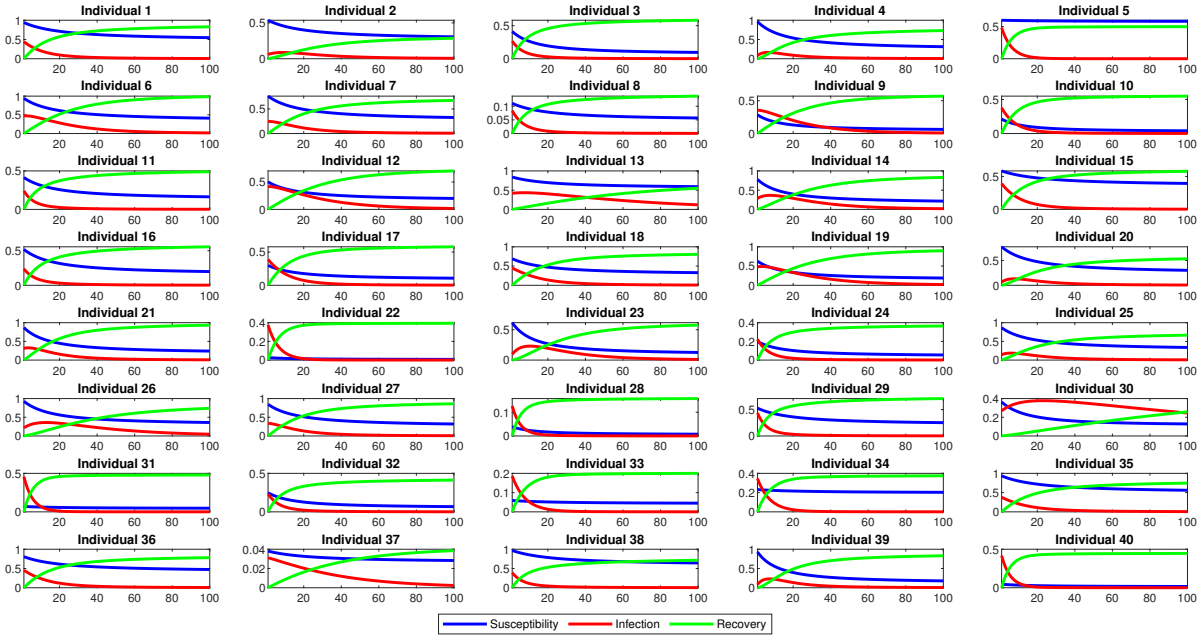

FIGURE 5. Simulation of the model for the group 2 with the control 1

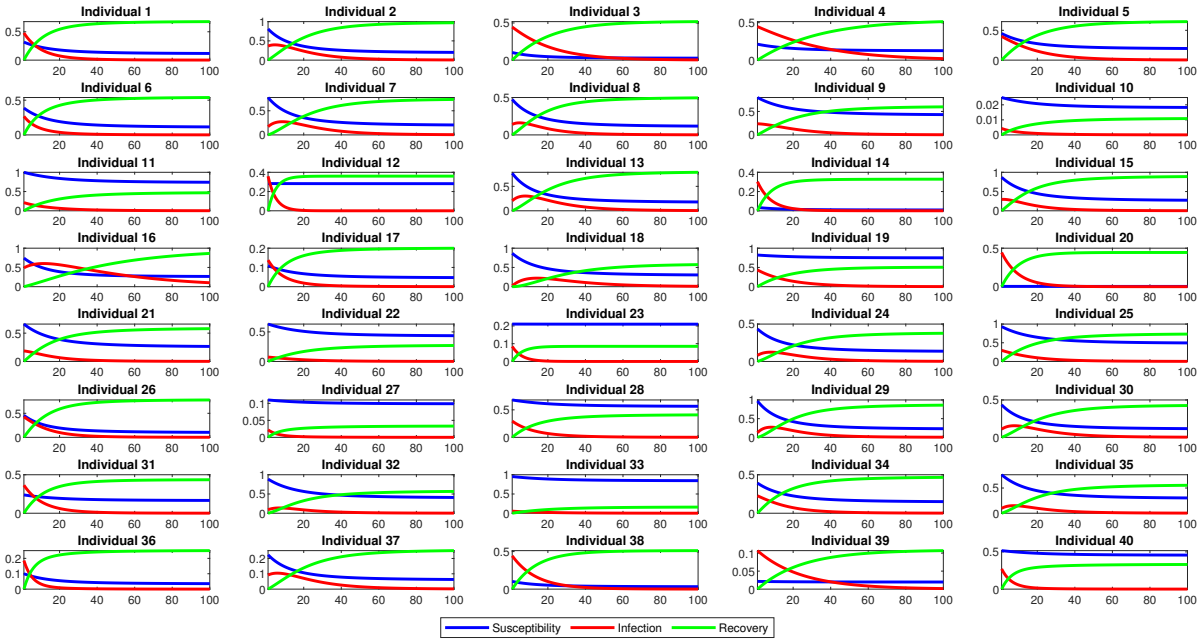

TABLE 2. Generated survival analysis data with control 1 for the group 1 and 2

Individual IDs	Group 1		Group 2	
	Time To Recovery	Recovery Status	Time To Recovery	Recovery Status
1	20	1	17	1
2	1	1	36	1
3	8	1	32	1
4	1	1	52	1
5	10	1	28	1
6	45	1	10	1
7	23	1	35	1
8	1	1	17	1
9	36	1	25	1
10	12	1	1	1
11	7	1	13	1
12	47	1	7	1
13	100	0	36	1
14	49	1	9	1
15	17	1	24	1
16	8	1	100	0
17	17	1	4	1
18	26	1	1	1
19	52	1	26	1
20	1	1	15	1
21	28	1	14	1
22	9	1	1	1
23	1	1	1	1
24	7	1	1	1
25	23	1	20	1
26	71	1	21	1
27	26	1	1	1
28	3	1	15	1
29	10	1	31	1
30	100	0	23	1
31	9	1	15	1
32	7	1	1	1
33	6	1	1	1
34	10	1	15	1
35	22	1	1	1
36	23	1	5	1
37	1	1	1	1
38	11	1	21	1
39	1	1	3	1
40	8	1	7	1

FIGURE 6. Survival curves with control u_1 (a) group 1 (b) group 2

(a)

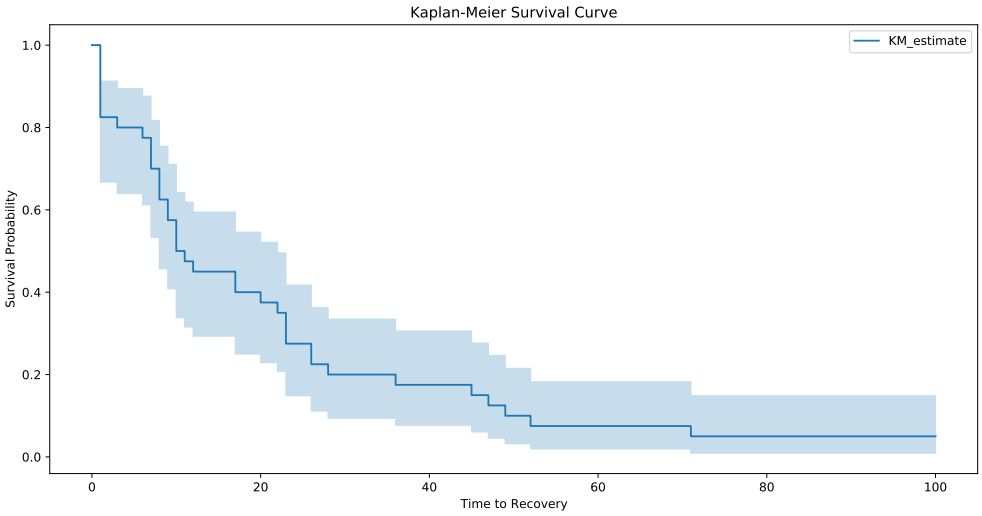

(b)

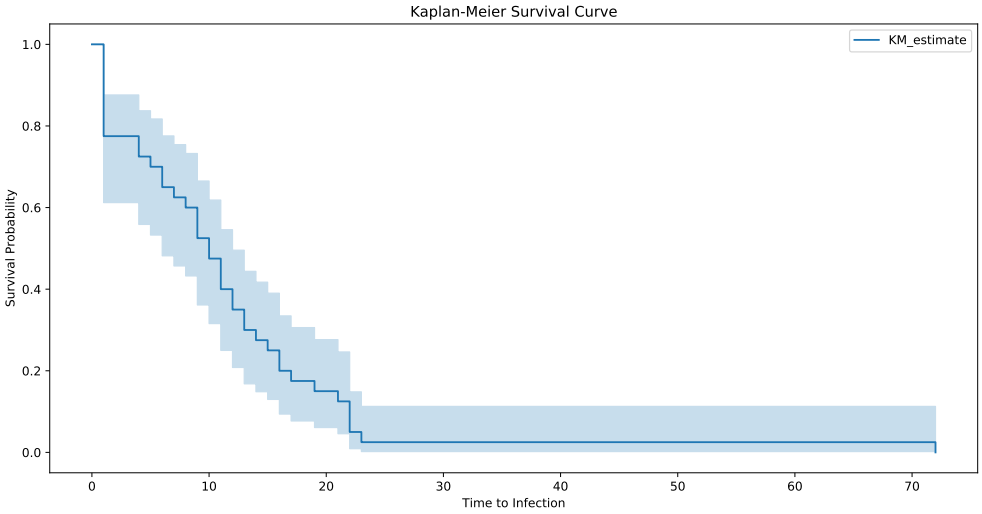

Figure 1 focuses on the first subgroup of 40 individuals in Group 1. These individuals undergo the simulation without any specific control measures. The subplots, numbered 1 to 40, offer a detailed view of the temporal evolution of these rates for each individual.

Similarly, Figure 2 concentrates on Group 2, specifically the first subgroup of 40 individuals. These individuals also undergo the simulation without any control measures, allowing for a comparative analysis with the corresponding subgroup in Group 1. The format and structure of Figure 2 mirror that of Figure 1, providing a parallel examination of susceptibility, infection, and recovery rates for each individual over time. The goal is to observe and compare trends between the two groups, shedding light on the inherent variability in infection dynamics.

Overall, the observed trend indicates that a significant majority of individuals within the simulated population exhibited disease symptoms and generated antibodies. A notable portion of the population experienced an extended duration before achieving recovery. This suggests that the infectious agent had a substantial impact on most individuals, prompting symptomatic responses and robust antibody production by the immune system. However, the prolonged recovery period for a small subset of individuals suggests variability in the duration required to fully overcome the infection. This diversity in recovery times emphasizes the nuanced nature of disease progression within the simulated population, highlighting the complex interplay between the infectious agent and individual immune responses.

This detailed visualization enables a thorough examination of how susceptibility, infection, and recovery change for each individual in the absence of control measures. Insights gained from these subplots can reveal patterns, variations, and potential high-risk periods for infection within this subgroup.

In Figure 3, we illustrate survival curves for two distinct subgroups, each consisting of 40 individuals as detailed in Table 1, with each subgroup represented in a subplot. Subplot (a) corresponds to Group 1, while subplot (b) represents Group 2. These curves visually depict the time until individuals in each subgroup transition from an infectious to a non-infectious state, without the influence of any control measures.

The survival curves show the proportion of individuals within each group who remain infectious over time. In the absence of controls, there is a gradual decline in the survival probability,

indicating a decreasing likelihood of individuals transitioning to a non-infectious state. The slower decline suggests that a considerable proportion of individuals remain infectious by the study's end, leading to a lower probability of transitioning to a non-infectious state as time progresses.

Both Group 1 and Group 2 exhibit similar trends without controls, with a significant portion of individuals succumbing to the infection over time. The decreasing survival probability reflects the cumulative effect of disease progression within each group.

It's important to emphasize that these survival curves serve as a baseline for comparison with scenarios involving control measures (u_1 and u_2). The divergence of survival curves between different groups and control strategies will offer insights into the effectiveness of interventions in influencing the duration of infectious periods and, consequently, the overall dynamics of disease spread within the simulated population.

Figures 4 and 5 provide a comprehensive visual representation of the dynamic interplay between susceptibility, infection, and recovery rates for individuals within Group 1 and Group 2, respectively, under the influence of control strategy u_1.

In each figure, the 40 subplots meticulously detail the temporal evolution of susceptibility, infection, and recovery rates for individual members of the respective groups. The introduction of u_1 adds complexity to the system. The figures aim to demonstrate individual-level responses to the applied control, providing insights into the treatment's effectiveness in influencing disease progression.

The outcomes depicted in Figures 4 and 5 reveal promising and overall positive results for individuals subjected to control strategy u_1. The notable observation is the substantial decrease in infection rates for nearly all individuals, with rates consistently dropping below 0.1 and trending toward zero as the observation period concludes.

The declining trend in infection rates clearly demonstrates the effectiveness of the implemented control measures, underscoring their capacity to reduce the spread of the modeled disease within the examined population. The convergence of infection rates towards zero at the conclusion of the observation period indicates a significant containment of the pathogen, contributing to a notable decrease in the prevalence of active infections.

Additionally, the prominently increased recovery rates, which indicate the proportion of individuals who have successfully defeated the infection, correspond closely with the decrease in infection rates. This reflects the individuals' capability to generate effective immune responses, leading to the alleviation of symptoms and eventual recovery. The substantial surge in recovery rates is a testament to the robust immune response induced by the control strategy, resulting in the successful recovery of a majority of individuals.

The observed high recovery rates signify not only the resolution of the infection but also the establishment of acquired immunity, affording individuals protection against potential future encounters with the modeled disease.

In Figure 6, we examine the Kaplan-Meier survival curves for two subgroups outlined in Table 2: (a) Group 1 and (b) Group 2, both under the influence of Control u_1. These curves portray the likelihood of individuals remaining infectious over time, taking into account the implemented control measures.

The survival curve for Group 1 shows a sharp decline, indicating a significant reduction in the duration of infectiousness among individuals with the application of Control u_1. The steep drop suggests a swift and effective response to the control measures, resulting in expedited recovery times and a decreased chance of remaining infectious. This observation aligns with the expectation that effective control measures can substantially influence the course of infection.

FIGURE 7. Simulation of the model for the group 1 with the control 2

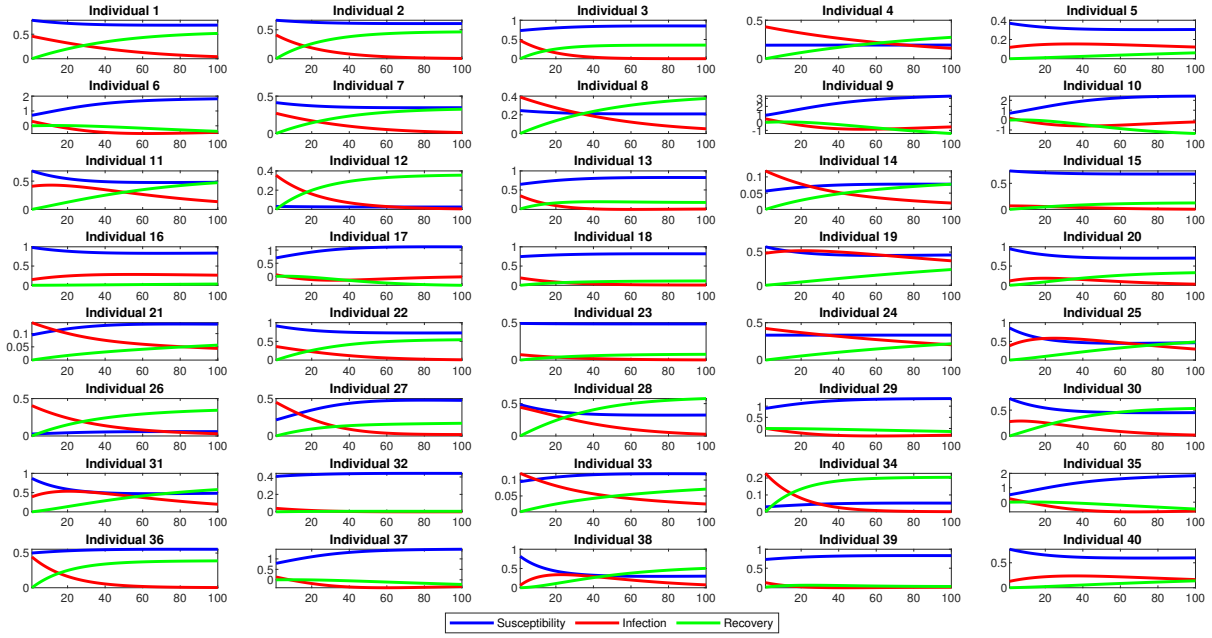

FIGURE 8. Simulation of the model for the group 2 with the control 2

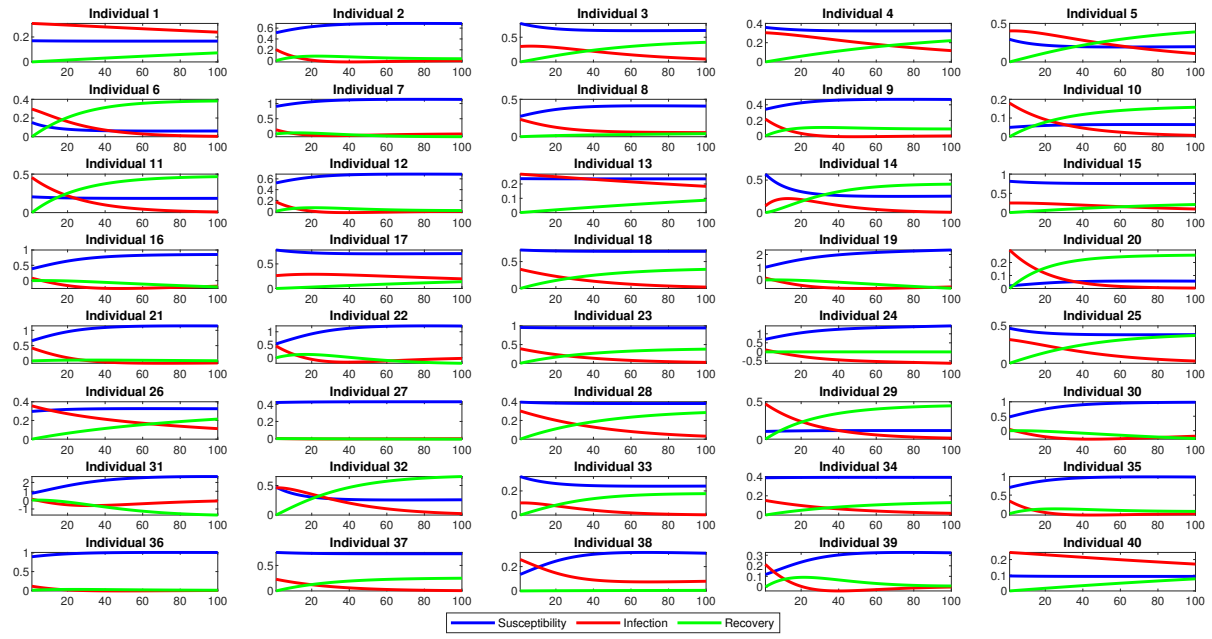

TABLE 3. Generated survival analysis data with control 2 for the group 1 and 2

Individual IDs	Group 1		Group 2	
	Time To Recovery	Recovery Status	Time To Recovery	Recovery Status
1	69	1	100	0
2	36	1	9	1
3	27	1	77	1
4	100	0	100	0
5	100	0	100	0
6	9	1	33	1
7	40	1	4	1
8	70	1	29	1
9	9	1	11	1
10	4	1	18	1
11	100	0	40	1
12	32	1	7	1
13	19	1	100	0
14	9	1	43	1
15	1	1	95	1
16	100	0	1	1
17	1	1	100	0
18	17	1	52	1
19	100	0	3	1
20	59	1	24	1
21	21	1	21	1
22	45	1	12	1
23	1	1	51	1
24	100	0	2	1
25	100	0	57	1
26	52	1	100	0
27	38	1	1	1
28	62	1	52	1
29	1	1	45	1
30	56	1	1	1
31	100	0	2	1
32	1	1	62	1
33	11	1	5	1
34	17	1	20	1
35	7	1	14	1
36	30	1	2	1
37	3	1	26	1
38	1	1	35	1
39	3	1	9	1
40	100	0	100	0

FIGURE 9. Survival curves with control u_2 (a) group 1 (b) group 2

(a)

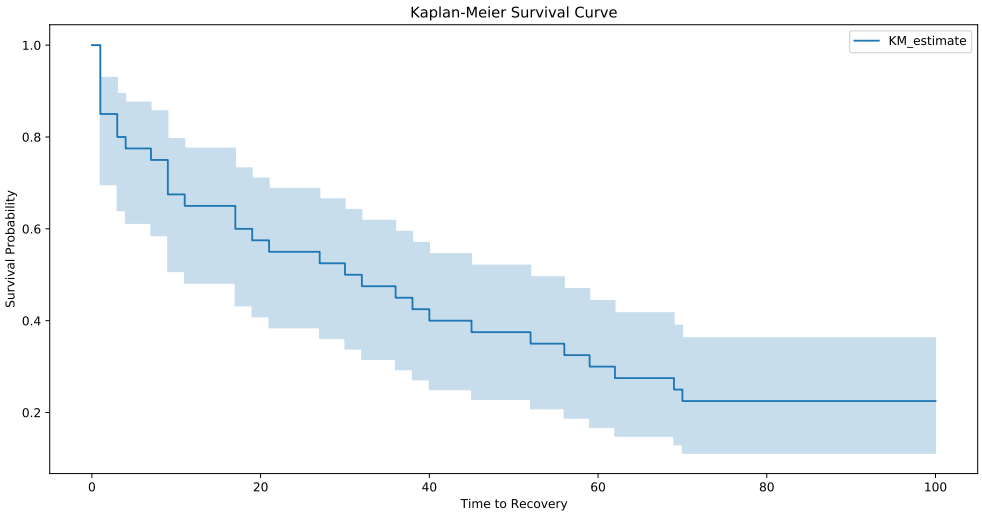

(b)

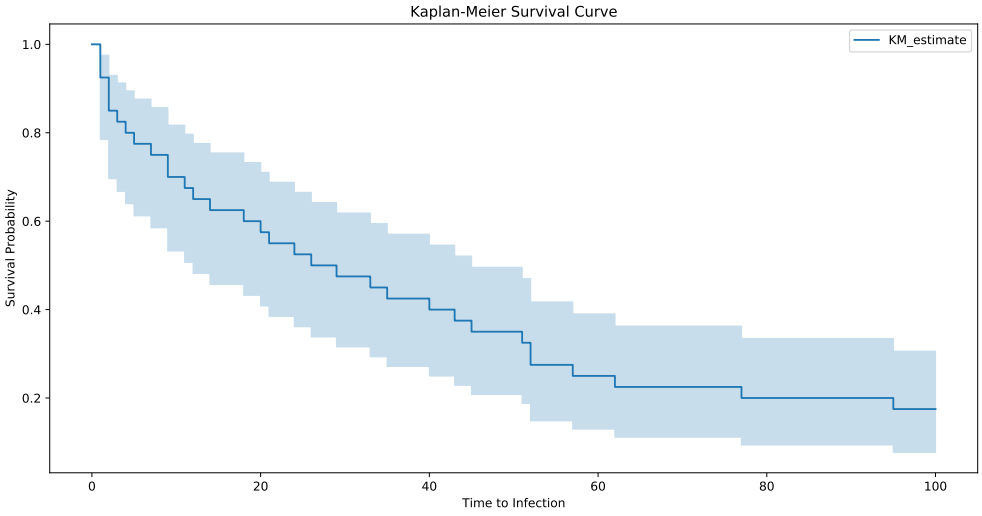

Similarly, in Group 2, the survival curve exhibits a pronounced and rapid decline, signaling a successful decrease in the duration of infectiousness with Control u_1. The quicker descent in this subgroup implies that the implemented control measures are effective across diverse populations, reinforcing the notion that the control strategy is impactful in varied settings.

In Figures 7 and 8, the impact of control strategy u_2 is depicted through 40 subplots, each detailing the dynamic evolution of susceptibility, infection, and recovery rates for individuals within Group 1 and Group 2, respectively, under the influence of u_2.

The key observation revolves around the distinct patterns of susceptibility and infection rates in response to control u_2. Unlike scenarios without controls, where infection rates surged and remained high for a significant period, the introduction of control u_2 markedly reduces both susceptibility and infection rates.

Control u_2, designed to enforce separation and awareness to promote cautionary measures, appears effective in mitigating the spread of the simulated disease. The decline in infection rates indicates a successful intervention in minimizing person-to-person transmission within the population. Additionally, the reduction in susceptibility rates underscores the preventive nature of u_2, decreasing the likelihood of individuals becoming infected.

Regarding recovery, the observed trends suggest a positive impact, albeit with variability among individuals. Recovery rates, indicative of successful outcomes in overcoming infection, exhibit a noticeable upward trend. This implies that under control u_2, a significant portion of individuals can effectively mount immune responses leading to recovery.

The interaction among susceptibility, infection, and recovery rates in the presence of control u_2 underscores its potential as a preventive measure. The decrease in infection rates and the simultaneous increase in recovery rates highlight the strategy's effectiveness in mitigating the impact of the simulated disease.

Overall, control u_2 leads to a significant reduction in susceptibility and infection rates, fostering a conducive environment for recovery. This outcome underscores the importance of separation and awareness as effective measures in disease control and may provide guidance for public health interventions, particularly in situations requiring cautionary measures and limited physical interaction.

In Figure 9, we analyze the Kaplan-Meier survival curves for two subgroups outlined in Table 3: (a) Group 1 and (b) Group 2, both subjected to Control u_2.

The survival curve for Group 1 under Control u_2 exhibits a swift decline, indicating a substantial decrease in the duration of infectiousness. Control u_2, incorporating measures like separation and awareness to promote caution, proves effective in accelerating recovery times and reducing the likelihood of individuals remaining infectious. The steep descent suggests that this control strategy significantly limits the spread of infection within Group 1.

Similarly, in Group 2, the survival curve demonstrates a rapid decline, underscoring the effectiveness of Control u_2 in reducing the duration of infectiousness. The curve's swift descent indicates the successful implementation of separation and awareness measures, resulting in expedited recovery times and decreased probabilities of individuals remaining infectious.

Contrasting the survival curves with Control u_2 to those without any controls highlights the substantial impact of implementing control measures. Notably, while the curves under Control u_2 decline swiftly, there is a discernible difference when compared to the curves under Control u_1, which exhibit an even faster decline. This comparison emphasizes the importance of assessing various control strategies to identify the most effective approaches for mitigating the impact of infectious diseases in diverse settings.

Tables 1, 2, and 3 offer a comprehensive overview of the simulated data derived from the SIR model, focusing on recovery dynamics within both Group 1 and Group 2. The data encompasses vital details such as individual IDs, time to recovery, and recovery status, with recovery defined as the point when the infection rate of individuals drops below 10%. Each table serves as an extensive record of the simulated scenarios, providing insights into the temporal aspects of recovery for each individual.

In Table 1, the emphasis lies on the initial subset of 40 individuals from both groups, representing scenarios without any controls. This enables an exploration of the inherent dynamics of recovery in the absence of specific interventions.

Table 2 delves into the recovery dynamics of the subsequent 40 individuals in both groups, where the control strategy u_1 is implemented. The inclusion of u_1 aims to evaluate the impact of specific treatment or medical intervention on the recovery timelines and statuses of individuals. This table facilitates a comparative analysis, illustrating how the introduction of u_1 influences the overall recovery process.

Similarly, Table 3 shifts the focus to the final 40 individuals in both groups, incorporating the control strategy u_2. This table sheds light on how non-pharmaceutical interventions such as separation and awareness impact recovery outcomes, offering insights into the efficacy of strategies that emphasize reducing interpersonal contact.

5.2. Comparison of Scenarios. In order to evaluate the statistical significance of the observed variations in survival among different scenarios, we performed a log-rank test. The log-rank test is a commonly employed statistical technique for comparing the survival curves of distinct groups. In our study, we utilized the log-rank test to compare the survival curves of individuals under different control scenarios.

$\boldsymbol{G}_1$ *without &* $\boldsymbol{G}_2$ *without.* Initially, our aim was to compare the survival curves for group 1 and 2 respectively, in the absence of controls. The log-rank test produced a test statistic of 0.49, indicating that there may not be a substantial difference in survival between the compared subgroups.

The corresponding p-value of 0.48 represents the probability of obtaining such results by random chance. A p-value below a chosen significance level (typically 0.05) indicates a statistically significant difference in survival between the compared scenarios.

The obtained p-value of 0.48 exceeds the conventional significance level. Consequently, we do not reject the null hypothesis. This implies that there is no significant difference in survival between the subgroups of 40 individuals from each group when there are no controls.

$\boldsymbol{G}_1$ *with* u_1 *&* $\boldsymbol{G}_2$ *with* u_1. When comparing the survival outcomes of 40 individuals from each group under the influence of control u_1, the log-rank test yielded a test statistic of 0.57, accompanied by a corresponding p-value of 0.44. This statistic, assessing the difference between observed and expected survival curves, pointed to a moderate discrepancy in survival experiences. However, with a p-value of 0.44 exceeding the common significance level of 0.05, there was insufficient evidence to reject the null hypothesis.

The $-\log_2(\mathrm{p})$ value of 1.15 further supports this interpretation, suggesting moderate evidence against the null hypothesis. These findings indicate that under the conditions of control u_1, there may not be a substantial divergence in survival outcomes among the studied subgroups.

$\boldsymbol{G}_1$ *with* u_2 *&* $\boldsymbol{G}_2$ *with* u_2. In the comparison of survival outcomes for the final subgroups, each comprising 40 individuals from both Group 1 and Group 2 under the influence of control u_2, the log-rank test generated a test statistic of 0.154537 and a p-value of 0.694237. This statistic, indicating the difference in survival experiences between the groups, was relatively small,

suggesting only a minimal dissimilarity. Furthermore, the p-value, significantly higher than the typical significance level of 0.05, signifies a lack of evidence to reject the null hypothesis.

The $-\log_2(\mathrm{p})$ value of 0.5265 further reinforces this interpretation, emphasizing the absence of a significant difference in survival outcomes. These findings imply that the implemented control u_2 might not have a substantial impact on the survival dynamics of the considered subgroups.

$\boldsymbol{G}_1$ *without &* $\boldsymbol{G}_1$ *with* u_1. The comparison between the initial 40 individuals from Group 1, without any controls, and the subsequent 40 individuals from the same Group 1 under control u_1 revealed a significant distinction in their survival experiences. The log-rank test produced a substantial test statistic of 33.15 and an extremely low p-value of 8.49×10^{-9}. This test statistic indicates a notable difference in survival outcomes between the two subsets, while the remarkably small p-value strongly refutes the null hypothesis of equal survival functions. The $-\log_2(\mathrm{p})$ value of 26.80 further emphasizes the strength of this result, highlighting a highly significant contrast in survival outcomes between the two situations. These results suggest that the introduction of control u_1 significantly influences survival dynamics, leading to a notable enhancement in survival rates for the latter subgroup of individuals from Group 1.

$\boldsymbol{G}_1$ *without &* $\boldsymbol{G}_1$ *with* u_2. In comparing the initial 40 individuals from Group 1 without controls to the final 40 individuals from the same Group 1 under control u_2, the log-rank test produced a test statistic of 5.920362. The associated p-value is 0.014967, with a $-\log_2(\mathrm{p})$ value of 6.062082. These findings indicate a statistically significant distinction in survival experiences between the two groups, suggesting that the introduction of control u_2 has a notable impact on survival rates. The low p-value and high $-\log_2(\mathrm{p})$ value provide strong evidence against the null hypothesis, supporting the notion that control u_2 influences survival outcomes in Group 1.

$\boldsymbol{G}_1$ *with* u_1 *&* $\boldsymbol{G}_1$ *with* u_2. In the comparison between the second set of 40 individuals from Group 1 under control u_1 and the last 40 individuals from the same Group 1 under control u_2, the log-rank test revealed a considerable test statistic of 7.268696 and a significantly low p-value of 0.007017. This test statistic indicates a notable difference in the survival experiences of the two subgroups, while the small p-value strongly refutes the null hypothesis of equal

survival functions. The corresponding $-\log_2(\mathrm{p})$ value of 7.154997 further underscores the robust significance of this finding, highlighting a substantial divergence in survival outcomes between the two scenarios. These results suggest that the implementation of control strategies u_1 and u_2 has distinct impacts on survival dynamics, with control u_1 demonstrating a more pronounced effect on improving survival rates compared to control u_2.

G$_2$ *without &* ***G***$_2$ *with* u_1. In the comparison between the initial 40 individuals from Group 2 without controls and the subsequent 40 individuals from the same Group 2 under control u_1, the log-rank test yielded noteworthy results. The computed test statistic is notably high at 34.532159, indicating a substantial difference in their survival experiences. The associated p-value is exceedingly low (4.192668e-09), strongly rejecting the null hypothesis of identical survival functions. The $-\log_2(\mathrm{p})$ value, reaching 27.829484, underscores the robust significance of these findings. These results suggest a pronounced impact of implementing control u_1, further emphasizing its effectiveness in enhancing survival rates within Group 2 compared to the absence of controls.

G$_2$ *without &* ***G***$_2$ *with* u_2. In the comparison between the initial 40 individuals from Group 2 without controls and the final 40 individuals from the same Group 2 under control u_2, the log-rank test resulted in a test statistic of 8.592951. The corresponding p-value is 0.003375 , and the $-\log_2(\mathrm{p})$ value is 8.211039 . These findings signify a statistically significant difference in survival experiences between the two groups. The low p-value and high $-\log_2(\mathrm{p})$ value suggest a strong rejection of the null hypothesis, supporting the notion that the implementation of control u_2 has a substantial impact on survival outcomes in Group 2.

G$_2$ *with* u_1 *&* ***G***$_2$ *with* u_2. The log-rank test results comparing the second set of 40 individuals from Group 2 under control u_1 with the last 40 individuals from the same Group 2 under control u_2 are noteworthy. The calculated test statistic is remarkably high at 11.030814, and the associated p-value is extremely low (0.000896). This substantial test statistic implies a significant difference in survival experiences between these two subgroups. The negligible p-value strongly rejects the null hypothesis, emphasizing the unequal nature of their survival functions. The $-\log_2(\mathrm{p})$ value, reaching 10.124056, underscores the robust significance of these results.

In essence, the findings suggest a distinct impact of control strategies u_1 and u_2 on survival dynamics, with control u_1 demonstrating a more pronounced effect in improving survival rates within Group 2 compared to control u_2.

Table 4 provides a comprehensive comparison of the effectiveness of control strategies, namely u_1 and u_2, on survival dynamics within distinct groups (Group 1 and Group 2). The presented test statistics, p-values, and corresponding $-\log_2(\mathrm{p})$ values highlight the impact of each control strategy on the survival rates of individuals in various scenarios.

Table 5 presents a cross-group comparison of the effectiveness of control strategies, u_1 and u_2, in influencing survival dynamics. The test statistics, p-values, and corresponding $-\log_2(\mathrm{p})$ values are provided for various scenarios, including comparisons between groups (Group 1 and Group 2) and different control strategies. The table aims to elucidate how the impact of control measures varies across distinct groups, contributing to a comprehensive understanding of survival dynamics in different contexts.

TABLE 4. Comparison of Control Strategies in Survival Analysis: Log-Rank test

	Group 1			
	G1 with u_1	**G1 with u_2**		**G1 with u_2**
G1 without	**Test:** 33.157297 **p-value:** 8.499681×10^{-9} $-\log_2(p)$**:** 26.809944	**Test:** 5.920362 **p-value:** 0.014967 $-\log_2(p)$**:** 6.062082	**G1 with u_1**	**Test:** 7.268696 **p-value:** 0.007017 $-\log_2(p)$**:** 7.154997
	Group 2			
	G2 with u_1	**G2 with u_2**		**G2 with u_2**
G2 without	**Test:** 34.532159 **p-value:** 4.192668×10^{-09} $-\log_2(p)$**:** 27.829484	**Test:** 8.592951 **p-value:** 0.003375 $-\log_2(p)$**:** 8.211039	**G2 with u_1**	**Test:** 11.030814 **p-value:** 0.000896 $-\log_2(p)$**:** 10.124056

TABLE 5. Cross-Group Comparison of Control Strategies in Survival Analysis

	G2 without	**G2 with u_1**	**G2 with u_2**
G1 without	**Test:** 0.495248 **p-value:** 0.481596 $-\log_2(p)$**:** 1.054105	**Test:** 48.860069 **p-value:** 2.748905×10^{-12} $-\log_2(p)$**:** 38.40428	**Test:** 8.631822 **p-value:** 0.003303 $-\log_2(p)$**:** 8.241828
G1 with u_1	**Test:** 26.58584 **p-value:** 2.520846×10^{-7} $-\log_2(p)$**:** 21.919589	**Test:** 0.572651 **p-value:** 0.449207 $-\log_2(p)$**:** 1.154546	**Test:** 6.046827 **p-value:** 0.013931 $-\log_2(p)$**:** 6.165525
G1 with u_2	**Test:** 6.263054 **p-value:** 0.012328 $-\log_2(p)$**:** 6.3419	**Test:** 12.996883 **p-value:** 0.000312 $-\log_2(p)$**:** 11.646121	**Test:** 0.154537 **p-value:** 0.694237 $-\log_2(p)$**:** 0.5265

6. CONCLUSION AND DISCUSSION

This study replicates real-world situations where various control measures are employed to address infectious diseases. The knowledge obtained from this study can guide public health strategies and assist in making decisions to manage the spread of infections in various environments.

In this extensive investigation, we utilized a multi-individual SIR model to replicate the transmission of infection within two distinct groups, each comprising 120 individuals. We assessed the effectiveness of two control strategies, labeled as u_1 and u_2, representing medical intervention and behavioral interventions, respectively. Our analysis encompassed susceptibility, infection, and recovery rates, alongside survival curves for various scenarios, providing a thorough evaluation of different control methods and their consequences.

The simulations unveiled a notable reduction in infection rates upon the implementation of both control strategies, affirming the efficacy of the measures in expediting recovery and curtailing the duration of infection. Particularly, control u_1, focusing on medical treatment, exhibited a swifter decline in infection rates compared to control u_2, underscoring its effectiveness in mitigating the spread of the infectious agent. The survival curves depicted how the controls influenced the duration of infectious periods, with control u_1 showing a more pronounced effect,

leading to a quicker decline in survival probabilities and indicating an expedited transition to a non-infectious state.

Statistical comparisons utilizing log-rank tests emphasized significant disparities in survival dynamics between groups and control strategies. The $-\log_2(\mathrm{p})$ values provided a measurable indicator of the magnitude of these differences. The comparison of $-\log_2(\mathrm{p})$ values consistently favored control u_1 over control u_2 in terms of impacting survival outcomes, suggesting that the medical treatment strategy had a more substantial statistical influence on enhancing survival rates within the studied groups.

While statistical significance holds importance, the practical implications of implementing control strategies should also be taken into account. The findings imply that, within the context of the studied scenario, a strategy centered around medical treatment (u_1) might offer greater effectiveness in reducing infection rates and improving survival outcomes compared to behavioral interventions (u_2).

It's crucial to acknowledge that our study operates on specific assumptions inherent in the SIR model. Real-world variations may necessitate additional considerations and adjustments. Moreover, our analysis assumes continuous and uninterrupted data collection, whereas in reality, challenges in data collection may affect the accuracy and completeness of observations.

CONFLICT OF INTERESTS

The authors declare that there is no conflict of interests.

REFERENCES

[1] O. Zakary, M. Rachik, I. Elmouki, On the analysis of a multi-regions discrete SIR epidemic model: an optimal control approach, Int. J. Dyn. Control. 5 (2016), 917–930. https://doi.org/10.1007/s40435-016-0233-2.

[2] M. Lhous, O. Zakary, M. Rachik, et al. Optimal containment control strategy of the second phase of the COVID-19 lockdown in Morocco, Appl. Sci. 10 (2020), 7559. https://doi.org/10.3390/app10217559.

[3] O. Zakary, S. Bidah, M. Rachik, et al. Mathematical model to estimate and predict the COVID-19 infections in Morocco: optimal control strategy, J. Appl. Math. 2020 (2020), 9813926. https://doi.org/10.1155/2020/9813926.

[4] I. Cooper, A. Mondal, C.G. Antonopoulos, A SIR model assumption for the spread of COVID-19 in different communities, Chaos Solitons Fractals 139 (2020), 110057. https://doi.org/10.1016/j.chaos.2020.110057.

[5] Z. Omar, S. Bidah, M. Rachik, The impact of staying at home on controlling the spread of COVID-19: strategy of control, Rev. Mex. Ingen. Biom. 42 (2021), 10–26. https://doi.org/10.17488/RMIB.42.1.2.

[6] Y.C. Chen, P.E. Lu, C.S. Chang, et al. A Time-Dependent SIR Model for COVID-19 With Undetectable Infected Persons, IEEE Trans. Netw. Sci. Eng. 7 (2020), 3279–3294. https://doi.org/10.1109/TNSE.2020.3024723.

[7] N.A. Kudryashov, M.A. Chmykhov, M. Vigdorowitsch, Analytical features of the SIR model and their applications to COVID-19, Appl. Math. Model. 90 (2021), 466–473. https://doi.org/10.1016/j.apm.2020.08.057.

[8] C. Lienhardt, From exposure to disease: the role of environmental factors in susceptibility to and development of tuberculosis, Epidemiol. Rev. 23 (2001), 288–301.

[9] J.C. Miller, Spread of infectious disease through clustered populations, J. R. Soc. Interface. 6 (2009), 1121–1134. https://doi.org/10.1098/rsif.2008.0524.

[10] O. Zakary, M. Rachik, I. Elmouki, A multi?regional epidemic model for controlling the spread of Ebola: awareness, treatment, and travel?blocking optimal control approaches, Math. Methods Appl. Sci. 40 (2016), 1265–1279. https://doi.org/10.1002/mma.4048.

[11] O. Zakary, M. Rachik, I. Elmouki, A new epidemic modeling approach: Multi-regions discrete-time model with travel-blocking vicinity optimal control strategy, Infect. Dis. Model. 2 (2017), 304–322. https://doi.org/10.1016/j.idm.2017.06.003.

[12] O. Zakary, A. Larrache, M. Rachik, et al. Effect of awareness programs and travel-blocking operations in the control of HIV/AIDS outbreaks: a multi-domains SIR model, Adv. Differ. Equ. 2016 (2016), 169. https://doi.org/10.1186/s13662-016-0900-9.

[13] O. Zakary, M. Rachik, I. Elmouki, On the impact of awareness programs in hiv/aids prevention: an sir model with optimal control, Int. J. Computer Appl. 133 (2016), 1–6.

[14] G. D'Arrigo, D. Leonardis, S. Abd ElHafeez, et al. Methods to analyse time-to-event data: the Kaplan-Meier survival curve, Oxid. Med. Cell. Longev. 2021 (2021), 2290120. https://doi.org/10.1155/2021/2290120.

[15] J. Kishore, M. Goel, P. Khanna, Understanding survival analysis: Kaplan-Meier estimate, Int. J. Ayurveda Res. 1 (2010), 274. https://doi.org/10.4103/0974-7788.76794.

[16] V.S. Stel, F.W. Dekker, G. Tripepi, et al. Survival analysis I: The Kaplan-Meier method, Nephron Clin. Pract. 119 (2011), c83–c88. https://doi.org/10.1159/000324758.

[17] K.J. Jager, P.C. van Dijk, C. Zoccali, et al. The analysis of survival data: the Kaplan?Meier method, Kidney Int. 74 (2008), 560–565. https://doi.org/10.1038/ki.2008.217.

[18] J. Xie, C. Liu, Adjusted Kaplan-Meier estimator and log?rank test with inverse probability of treatment weighting for survival data, Stat. Med. 24 (2005), 3089–3110. https://doi.org/10.1002/sim.2174.

[19] P. Schober, T.R. Vetter, Kaplan-Meier curves, log-rank tests, and cox regression for time-to-event data, Anesth. Analg. 132 (2021), 969–970. https://doi.org/10.1213/ane.0000000000005358.

[20] J.K. Baird, S. Masbar, H. Basri, et al. Age-dependent susceptibility to severe disease with primary exposure to plasmodium falciparum, J. Infect. Dis. 178 (1998), 592–595. https://doi.org/10.1086/517482.

[21] N. Becker, J. Angulo, On estimating the contagiousness of a disease transmitted from person to person, Math. Biosci. 54 (1981), 137–154. https://doi.org/10.1016/0025-5564(81)90081-x.

[22] K.R. Kumar, M. Iyapparaja, V.R. Niveditha, et al. Monitoring and analysis of the recovery rate of Covid-19 positive cases to prevent dangerous stage using IoT and sensors, Int. J. Pervas. Comput. Commun. 18 (2020), 365–375. https://doi.org/10.1108/ijpcc-07-2020-0088.

[23] F. Qin, Q. Lv, W. Hong, et al. Association between CD4/CD8 ratio recovery and chronic kidney disease among human immunodeficiency virus-infected patients receiving antiretroviral therapy: A 17-year observational cohort study, Front. Microbiol. 13 (2022), 827689. https://doi.org/10.3389/fmicb.2022.827689.